Exploring of Be$_{1-x}$Cr$_x$Se alloys for spintronics and optoelectronic applications

H. Ambreen[a], S. Saleem[a], S. A. Aldaghfag[b], M. Zahid[c], S. Noreen[c], M. Ishfaq[a], M. Yaseen[a,*]
[a]*Spin-Optoelectronics and Ferro-Thermoelectric (SOFT) Materials and Devices Laboratory*, *Department of Physics, University of Agriculture, Faisalabad 38040, Pakistan*
[b]*Department of Physics, College of Sciences, Princess Nourah bint Abdulrahman University, P. O. Box 84428, Riyadh 11671, Saudi Arabia*
[c]*Department of Chemistry, University of Agriculture Faisalabad, Faisalabad 38040, Pakistan*

In this study, spin polarized density functional theory (DFT) is implemented to predict physical characteristic of Be$_{1-x}$Cr$_x$Se (x = 6.25%, 12.5%, 18.75%, 25%) compound. The electronic characteristics of pure BeSe compound show semiconductor behavior but after Cr doping BeSe elucidate half-metallic ferromagnetism (HMF) for all doping concentrations. The outcomes elucidate the total magnetic moment M$_{Tot}$ per Cr-atom are 4.0028, 4.0027, 4.0021 and 4.0002 μB for 6.25%, 12.5%, 18.75%, 25% concentrations, respectively and the magnetism mainly originated from *d*-state of the impurity atom which is further ensured from the magnetic spin density. Furthermore, the optical parameters are also computed to determine the effect of doping on the material's response to incident light of energy spanning from 0 to 10 eV. The optical study depict that the studied systems possess maximum absorbance and optical conductivity in UV-range with minimal reflection. The overall outcomes illustrate that the Cr doped beryllium selenide (BeSe) is promising material for spintronic and optoelectronic devices.

1. Introduction

From past few decades, an intensive experimental and theoretical work is done on an emergent group of compounds which is recognized as the dilute magnetic semiconductors (DMS). DMS has use in spintronic industry and multifunctional electronic devices (optoelectronics, gas sensors, field-emission devices, non-volatile memory devices and ultraviolet absorbers) [1-6]. The DMS are based on III–V and II–VI binary compounds which is the combination of both ferromagnetic (FM) and semiconducting properties. The DMSs are attained by incorporation of transition metals (TM) within host material's matrix [7] which changes the E$_g$ of host system due to change in electronic features [8] causing asymmetric band profiles showing metallic and semiconductive behavior in either spin channels leading to half metallic ferromagnetic materials. In 1983, HMF behavior was observed by De Groot *et al*. for the very first time, by studying band structures of half-Heusler compound such as PtMnSb and NiMnSb [9]. Several researchers have been predicted theoretically as well as experimentally, the behavior of HMF in various types of materials such as perovskite compounds La$_{0.7}$Sr$_{0.3}$MnO$_3$ [10], Heusler alloys Co$_2$MnSi [11], double perovskites Sr$_2$FeMoO$_6$ [12], also in binary compound like Cr-doped ZnTe [13], Cr-based BeTe, BeSe [14], V doped MgSe/MgTe [15], BeTe [16], ZnSe [17] and ZnTe [18].

In this respect, beryllium chalcogenides BeX (X= Se, S, Te) have garnered intense attention of scientific community due to their technological applications in optoelectronics, spintronics and micro-electronics [19-23] devices. At ambient pressure and temperature, BeX are

---

transformed from zinc blende to NiAs structure [24, 25]. These semiconductors have a wide E_g, large hardness, stability and maximum value of the bulk modulus [26]. Numerous current studies concentrated on electronic characteristics to attain FM properties and HM ferromagnetism in TM based BeSe compounds [27][28]. Moreover, the previous theoretical studies have been explored for $Be_{1-x}Mn_xX$ (X= S, Se, Te) [29, 30], Cr doped BeX (X= Se, Te) [31] and Cr doped PbSe [32], Mn doped CdS [33] compounds for realizing ferromagnetism.

In recent research optical, electronic, and magnetic characteristics of pure and $Be_{1-x}Cr_xSe$ at different concentration are systematically investigated by using FP-LAPW method. Results revealed that the probed alloy has a HM-behavior and good ferromagnetism. Literature survey revealed the limited computational work on doped BeSe compound. These outcomes may give a new route for implementation of investigated alloys in optoelectronic/spintronic devices.

2. Computational details

Based on the DFT, the WIEN2k code was used to explore the electronic, magnetic and optical characteristics of $Be_{0.9375}Cr_{0.0625}Se$ $Be_{00875}Cr_{0.125}Se$, $Be_{0.8125}Cr_{0.1875}Se$, and $Be_{0.75}Cr_{0.25}Se$. All the calculations are done with the help of FP-LAPW approach [34]. The electron-core interaction was described through generalized gradient approximation (GGA) which is parameterized by Perdew Burke Ernzerhof (PBE). In these calculations, the unit cell is portioned into two parts, for atomic spheres, the spherical harmonic expansion is used and for outside of the muffin tin (MT) sphere, the potential is constant owing to plane wave solutions of the Schrodinger wave equation. The MT sphere radius is taken in such a way that leakage charge should be zero. For non-overlapping spheres, the values of the muffin tin radii (R_{MT}) are selected as 2.23, 2.11, 2.98 (bohr) for elements of Cr, Be and Se, respectively. The convergence parameters $R_{MT} \times K_{max} = 8$ are used to converge the calculations. R_{MT} has the lowest value and K_{max} represents the high magnitude which used in plane wave expansion with angular momentum l_{max} and Gaussian factor G_{max} are 10 and 16, respectively. A 12 x 12 x 12 k-mesh is found to be well converged within first Brillouin zone (BZ). Furthermore, 1000 k-points are used within wedge of the first BZ to attain self-consistency. Threshold energy is selected as 10^{-6} Ry, to separate the core/valance electrons.

3. Results and discussions

3.1. Electronic and Magnetic Properties

The study of electronic characteristics comprises of spin-dependent band structure (BS) and density of states. The knowledge of BS is important to recognize compounds for their usage in electronic gadgets as it reveals the nature of the material (metal, insulator or semiconductor) [35]. Bands in solids arise owing to the electron's diffraction within periodic crystal lattice [36]. In literature, it is found that pure BeSe has the indirect E_g (2.43 eV) [37]. The intrinsic BeSe executes semiconductor behavior with indirect band gap 2.55 eV which is comparable to the reported work (see Fig. 1). Moreover, the clear view about the electronic structure is obtained through DOS. To understand the participation of various atoms, the behavior of the total DOS is examined (see Fig. 2a, b). The plots exhibit the same behavior that explained earlier described in BS. For more elaboration of total DOS, the spectra of partial DOS are computed (see Fig. 2c) which define the participation of s, p, d and f-orbitals of material. It is clear that the VB is majorly composed of Se-p atom around the Fermi-level (E_f) whereas the CB is contributed by Be-s and Se-p states with sharp peak that appeared at 6 eV and strong hybridization occurred due to these states. Moreover, it is observed that there is no spin polarization in pure BeSe compound. After doping, the BeSe compound is polarized in both spins (down/ up). It revealed the semiconductor nature in spin-down channel with 2.38, 2.58, 2.8 and 2.93 eV E_g at 6.25%, 12.5%, 18.75% and 25% concentration while metallic behavior is observed in spin-up channel which confirm the HMF characteristic of the compound that leads to 100% spin-orientation at E_f (See Fig. 3(a-d)). At different concentrations, there are new states near the E_f and directly affect the electronic structure

of intrinsic BeSe system. The diversity of E_g designates the materials efficiency in spintronic gadgets.
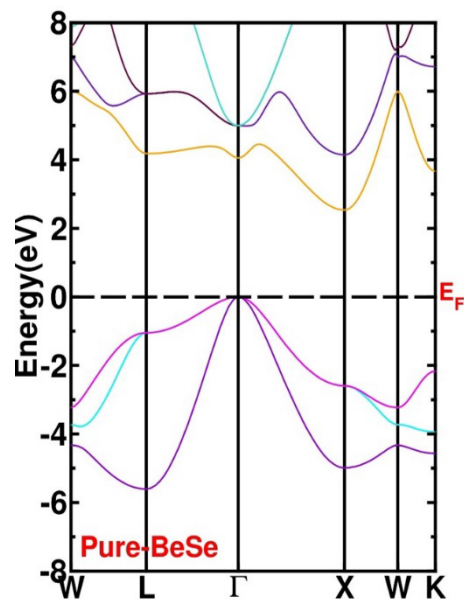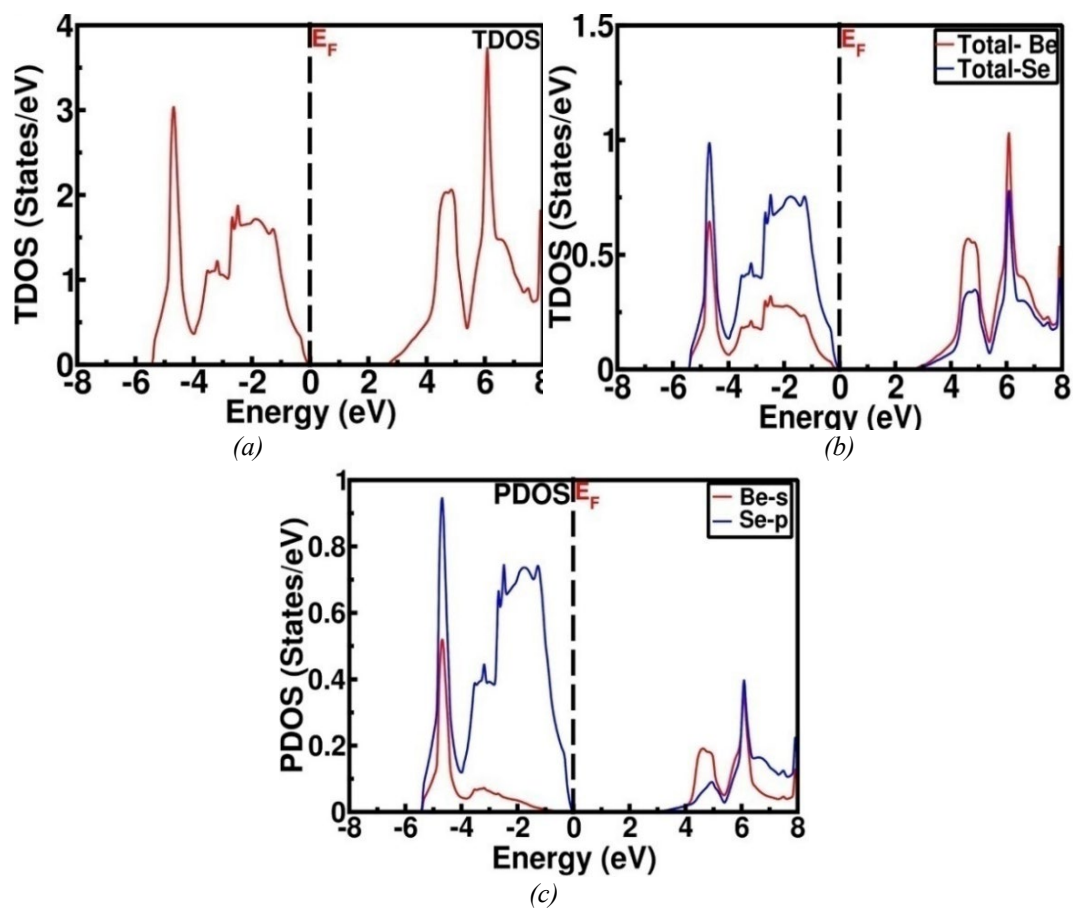

Fig. 1. BS plot of pure BeSe.

Fig. 2. (a) TDOS of BeSe compound (b) TDOS of elements and (c) PDOS plots of BeSe.
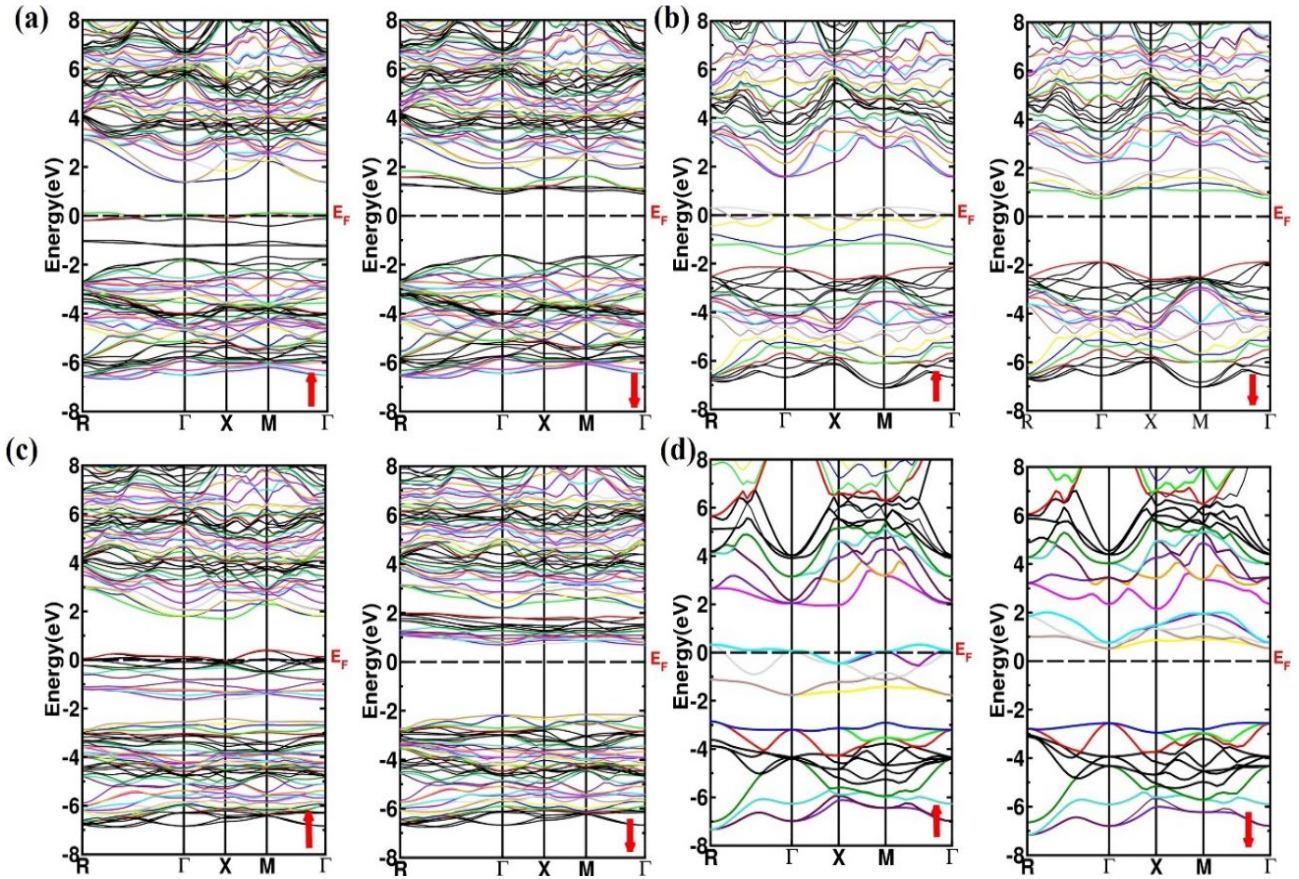
Fig. 3. BS of Be$_{1-x}$Cr$_x$Se at (a) Be$_{0.9375}$Cr$_{0.0625}$Se (b) Be$_{00875}$Cr$_{0.125}$Se (c) Be$_{0.8125}$Cr$_{0.1875}$Se (d) Be$_{0.75}$Cr$_{0.25}$Se.

To verify the cause of change in BS after doping, the TDOS and PDOS are also calculated (see Fig. 4). In doped compound, hybridization provokes the double exchange interaction that induces FM behavior. At x = 0.0625, 0.125 and 0.1875 doping content, the upper and lower VB region are within -2.4 to -7.2 eV and -2 to -7 eV, respectively which are largely contributed by Se-p/Cr-d ion with minor participation of Be-s/Cr-p states. In both spin versions (See Fig 4(a-c)), the sharp peak observed at 4.1 eV due to Be-s state. It is clearly showed that there exists a strong hybridized states above E$_f$ consisting of Cr/Se-p states and Cr-d state. In contrast with increasing doping concentration (x=25%), the d-orbital of the Cr-atom split into both e$_g$ and t$_{2g}$ orbitals. The five-fold degenerate TM-d state split into three-fold t$_{2g}$ (d_{xy}, d_{yz} and d_{xz}) bonding states and two-fold (d^2z and dx^2-y^2) anti-bonding states in accordance with the crystal field. Due to less coulomb interactions the e$_g$ orbitals are higher in energy than t$_{2g}$ states.

The valance region is mainly composed of TM-d (e$_g$ and t$_{2g}$) and Se-p states whereas in conduction region, the Cr-d_{t2g} state is large contribute near the E$_f$ in spin-dn channel (See Fig. 4d). Thus, doping element in BeSe compound is responsible for the usage of Be$_{1-x}$Cr$_x$Se compounds in spintronic gadgets. To confirm the thermodynamical stability of Be$_{1-x}$Cr$_x$Se compound, enthalpy of formation (ΔH) energy is calculated (see Table. 1) through the following relation [38, 39].

$$\Delta H = E_{\text{Be1}-\text{xCrxSe}} - aE_{Cr} - bE_{Be} - cE_{Se} \qquad (1)$$

The stability of the material is proved with negative value of ΔH. The negative sign illustrate that the energy is released to the environment during the formation of investigated compounds.

Table 1. Formation energy calculated for $Be_{1-x}Cr_xSe$ compound.

Cr-Concentration	$Be_{0.9375}Cr_{0.0625}Se$	$Be_{00875}Cr_{0.125}Se$	$Be_{0.8125}Cr_{0.1875}Se$	$Be_{0.75}Cr_{0.25}Se$
Formation Energy (ΔE_f)	-1.74	-1.81	-2.1	-2.4
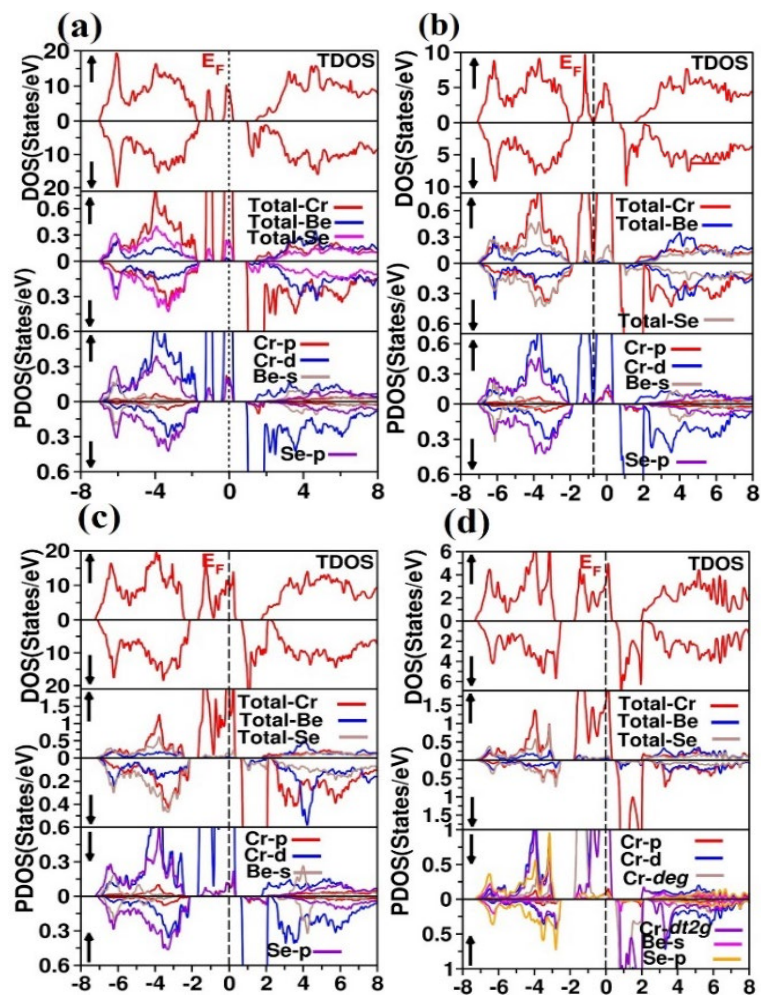
Fig. 4. Spin polarized DOS of $Be_{1-x}Cr_xSe$ at (a) $Be_{0.9375}Cr_{0.0625}Se$ (b) $Be_{00875}Cr_{0.125}Se$
(c) $Be_{0.8125}Cr_{0.1875}Se$ (d) $Be_{0.75}Cr_{0.25}Se$.
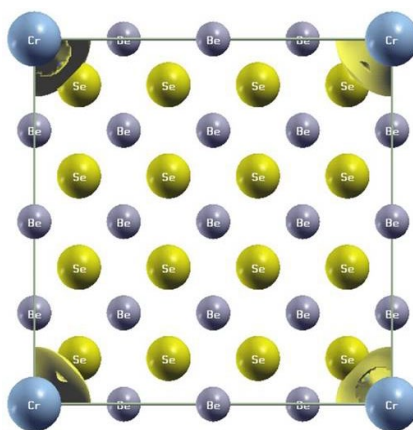
Fig. 5. Magnetic density of $Be_{1-x}Cr_xSe$ at x= 0.0625.

The computed net spin magnetic moments µB for Cr doped BeSe in interstitial zone and individual µB of Cr, Be and Se is summarized in Table 2. The strong magnetic moment is caused by the partially filled d-orbital at the Cr-site while the week hybridization between non-magnetic Cr-p and Be-s states is responsible for the minimum magnetic moment. Furthermore, spin-dependent density is calculated to ensure magnetism (see Fig. 5) in doped compounds. The calculated M_{Tot} of doped BeSe at x = 0.0625, 0.125, 0.1875 and 0.25 are 4.0028, 4.0027, 4.0021 and 4.0002 µB, correspondingly. Moreover, it is found that, atomic moment of Se-atom has negative sign favor antiparallel alignment whereas parallelly aligned Cr and Be atomic moment that have positive sign.

Table 2. Computed interstitial, local, and total magnetic moments of Cr doped BeSe.

Concentration	Magnetic Moment (µB)				
	Total	Interstitial	Cr	Be	Se
$Be_{0.9375}Cr_{0.0625}Se$	4.0028	0.77479	3.01124	0.06028	-0.00075
$Be_{00875}Cr_{0.125}Se$	4.0027	0.76910	3.03295	0.11074	-0.0018
$Be_{0.8125}Cr_{0.1875}Se$	4.0021	0.78411	3.10905	0.16509	-0.00477
$Be_{0.75}Cr_{0.25}Se$	4.0002	0.75869	3.06468	0.06489	-0.00445

3.2. Optical properties

The optical characteristics define the response of material to the incident light that based on the rate of electronic transitions and recombination in the desired spectral zone. The transitions in optical features are split into intra-band and interband transitions. In semiconductor materials, only interband transitions play vital role whereas for metals intraband transition is important [40]. The optical features of the compounds in response to light have been investigated within 0-10 eV. The dielectric constant ($\varepsilon_1(\omega)$ and $\varepsilon_2(\omega)$) is directly linked to BS and define the optical material's response to incident energy (E= hf) [36]. $\varepsilon_1(\omega)$ explain the dispersion of the incident photons while the $\varepsilon_2(\omega)$ is linked with BS of the materials and explains its absorptive behavior [41]. The static dielectric function $\varepsilon_1(0)$ for pure and $Be_{1-x}Cr_xSe$ (x= 6.25%, 12.5%, 18.75% and 25%) are computed as 6.5, 21.8, 28.1, 80.7, 58.1, respectively (See Fig. 6a). Its value decreases with increasing energy but after 6 eV its values become constant for all concentrations. Numerous researchers investigate the $\varepsilon_1(0)$ of similar compounds. Cobalt doped CdX (X = Te, Se, S) have values of ($\varepsilon_1(0)$) 25.67, 70.50 and 59.97, respectively [42] and $Be_xCd_{1-x}Se$ have $\varepsilon_1(0)$ values of 6.75, 6.66, 6.45, 6.36 and 6.21 at x = 0, 0.25, 0.50, 0.75, 1.0, correspondingly [43]. At 18.75% doping concentration, the $\varepsilon_1(\omega)$ attains negative values at 0.5 electron volt that indicate the reflecting (metallic) nature of the studied compound [38]. The low energy values associated with metallic nature and electrons are transmitted to intra-band regions. According to BS calculations, the values of $\varepsilon_1(0)$ and E_g are in agreement according to Penn's model, which suggest that $\varepsilon_1(0) \approx 1 + (\hbar\omega_p/E_g)^2$ [44], here, ω_p represent plasma resonance frequency. The interband transitions are expressed in $\varepsilon_2(\omega)$ and provide information about threshold energy points of the materials [45]. The $\varepsilon_2(\omega)$ for pure BeSe starts at 3.3 eV which corresponds to the electronic E_g. This threshold values mainly comes from the electronic transitions among VB (occupied states) and CB (un-occupied states). The critical points of $\varepsilon_2(\omega)$ occurs at 4, 3.1, 2.7 and 2.3 eV for $Be_{0.9375}Cr_{0.0625}Se$ $Be_{00875}Cr_{0.125}Se$, $Be_{0.8125}Cr_{0.1875}Se$, and $Be_{0.75}Cr_{0.25}Se$, respectively (See Fig. 6b). The absorption of light is maximum within energy span 5.4-6.9 eV, showing that the studied material could be suitable in optical devices. The coefficient of optical absorption $\alpha(\omega)$ of a semiconductor is a measure of amount of photon energy captivated by the material at a certain frequency. The onset edges of $\alpha(\omega)$ are used to obtain the optical band gap [45]. It takes key part in defining the competence of optoelectronic devices. The maximum absorption for pure BeSe compound is around 6 eV (156×10^4 cm^{-1}) in the UV region (See Fig. 6c). After doping, the values of the $\alpha(\omega)$ for 0.0625, 0.125, 0.1875 and 0.25 are 186×10^4, 175×10^4, 173×10^4 and 171×10^4 cm^{-1} at 6.4, 6.6, 6.9 and 7 eV, correspondingly, which means that the doping decreases the sharpness of the peaks. Thus, the resultant material is good absorbent of UV-light.

The σ(ω) explains the performance of a compound to conduct electrical current in response to an incident EM wave. It follows the same trend as depicted in α(ω). There exists no conductivity up to 2.63 eV that is equivalent to computed E_g. The magnitude of highest peaks (in visible-UV region) is 16495, 14871, 12735, 11538, 9700 $(\boldsymbol{\Omega}cm)^{-1}$ at photon energies 5.9, 6.1, 6.3, 6.5 and 6. 6 eV for pure, 6.25%, 12.5%, 18.75% and 25% concentrations, correspondingly (See Fig. 6d) which indicates that studied material is potential candidate for optoelectronic gadgets.
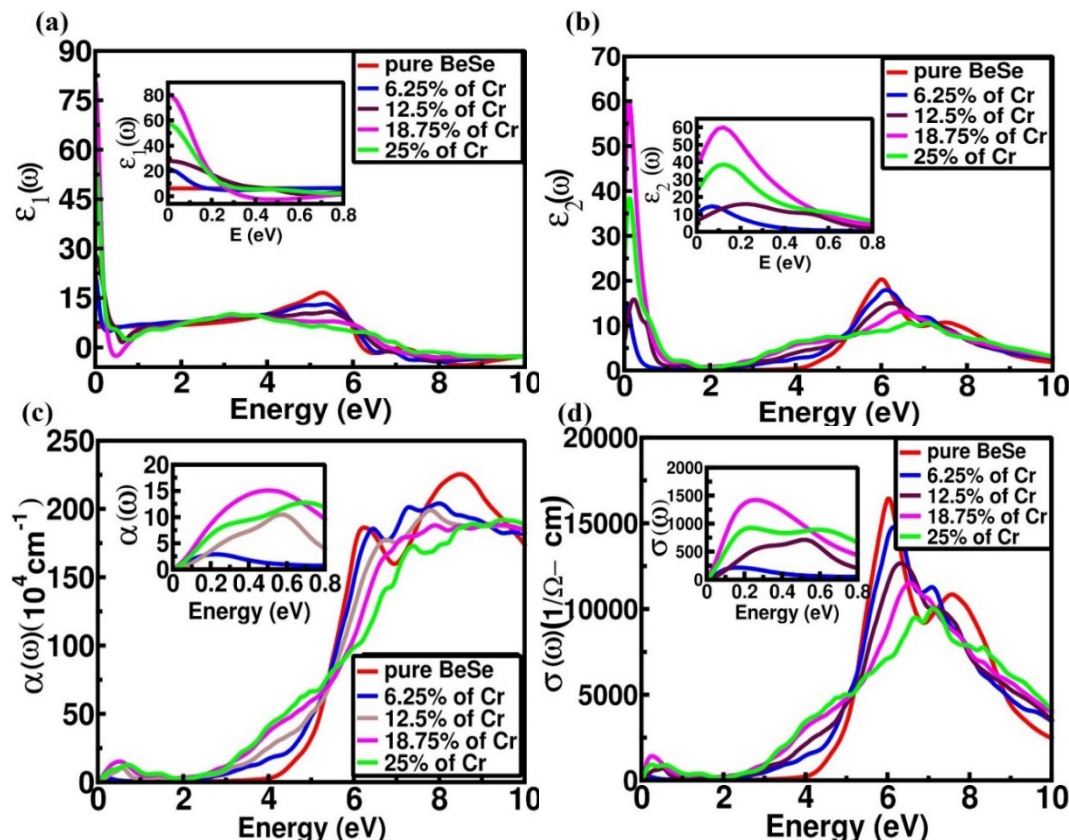

Fig. 6. (a) $\varepsilon_1(\omega)$, (b) $\varepsilon_2(\omega)$, (c) $\alpha(\omega)$ and $\sigma(\omega)$ of Cr doped BeSe.

The refractive index $n(\omega)$ determines speed of light in medium compared to speed of light in a vacuum [46]. The static $n(\omega)$ is 2.5 for pure BeSe compound but after doing its value is 4.8, 5.3, 9.2 and 7.7 for corresponding doped systems (see Fig. 7a) and these values start to decrease after 6.1 eV. The mathematical relation between $n(\omega)$ and $\varepsilon_1(\omega)$ is $n^2 - k^2 = \varepsilon_1(\omega)$ [45]. Another optical parameter is extinction coefficient $k(\omega)$ that is directly linked to $\alpha(\omega)$ [47, 48] through the following relationship $\alpha(\omega) = 4\pi k(\omega)/\lambda$ (see Fig. 6c). $k(\omega)$ is a measure of the diminution of photons (k > 0) in crystal due to absorption and scattering [49]. The $k(\omega)$ can be explained using the following formula.

$$k(\omega) = \frac{1}{\sqrt{2}}\left((\varepsilon_1^2(\omega) + \varepsilon_2^2(\omega))^{\frac{1}{2}} - \varepsilon_1(\omega)\right)^{\frac{1}{2}} \qquad (2)$$

For 18.75% doping concentration, the static $k(\omega)$ is 4.2 (see Fig. 7b) and reveal maximum peak at 0.2 eV as compared to other doping concentration. The $R(\omega)$ investigates the surface's nature of considered alloys. The static $R(\omega)$ are 0.1, 0.44, 0.48, 0.67 and 0.61 for x=0%, 6.25%, 12.5%, 18.75% and 25%, respectively (See Fig. 7c). $R(\omega)$ value exists at 0 eV owing to the lattice vibrations in the unit cell.
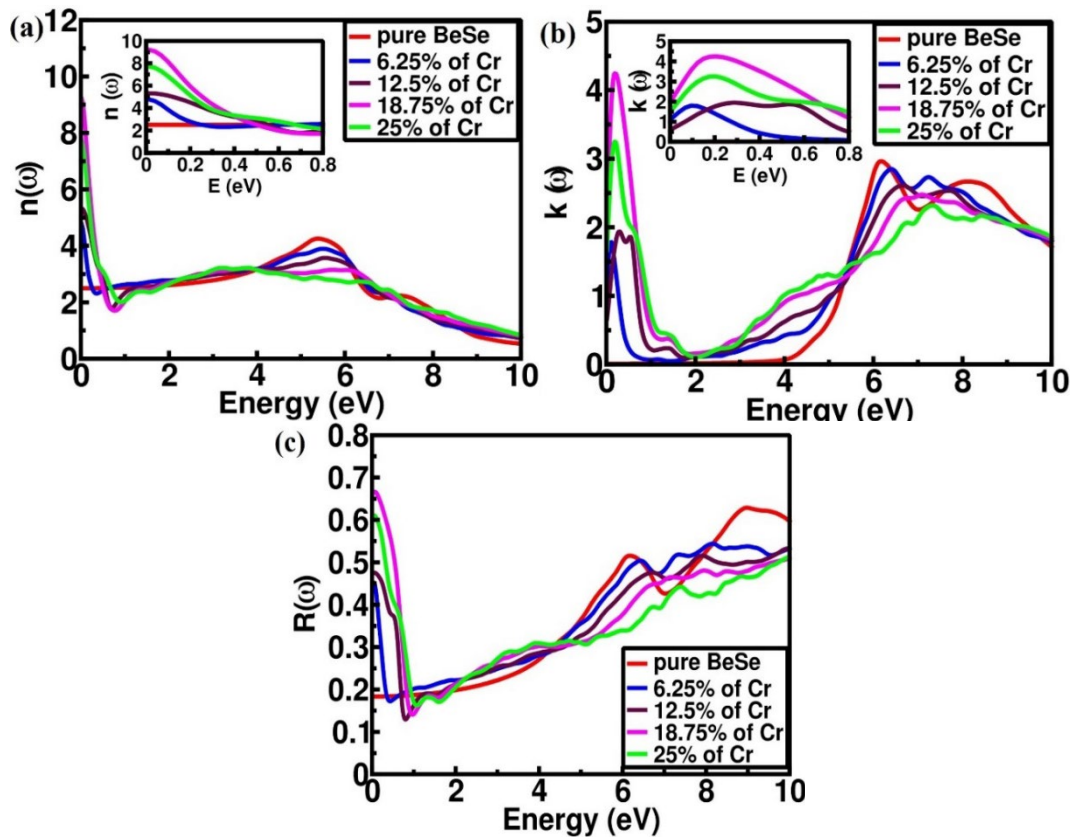
Fig. 7. (a) n(ω), (b) k(ω) and (c) R(ω) of Be$_{1-x}$Cr$_x$Se of Cr doped BeSe.

4. Conclusion

The spin-dependent optoelectronic and magnetic characteristics of Be$_{0.9375}$Cr$_{0.0625}$Se Be$_{00875}$Cr$_{0.125}$Se, Be$_{0.8125}$Cr$_{0.1875}$Se, and Be$_{0.75}$Cr$_{0.25}$Se alloys are studied by employing FP-LAPW approach. The analysis of electronic characteristics including BS and DOS depict semiconducting nature for pure BeSe compound and HMF behavior for different doping concentrations of Cr with 100% spin polarization. The M$_{Tot}$ is estimated to be 4.0028, 4.0027, 4.0021 and 4.0002 μB for Be$_{0.9375}$Cr$_{0.0625}$Se Be$_{00875}$Cr$_{0.125}$Se, Be$_{0.8125}$Cr$_{0.1875}$Se, and Be$_{0.75}$Cr$_{0.25}$Se, correspondingly which mainly come from TM-atoms Cr (confirmed through spin magnetic density) and minor magnetic moment with Be and Se-sites. Moreover, the optical parameters are also computed within energy range 0-10 eV and studied materials exhibit maximum absorption (at 6 eV) in UV-region. Results depict that the Cr doped beryllium selenide (BeSe) seems to be suitable candidate for spintronic and UV devices.

References

[1] A. Moezzi, A. M. McDonagh, M. B. Cortie, Chemical engineering journal, 185, 1-22 (2012); https://doi.org/10.1016/j.cej.2012.01.076

[2] D. Chu, Y. Masuda, T. Ohji, K. Kato, Langmuir, 26(4), 2811-2815 (2010); https://doi.org/10.1021/la902866a

[3] N. B. Brandt, V. V. Moshchalkov,Advances in Physics, 33(3), 193-256 (1984); https://doi.org/10.1080/00018738400101661

[4] J.K. Furdyna, Journal of Vacuum Science & Technology A: Vacuum, Surfaces, and Films, 4(4), 2002-2009 (1986); https://doi.org/10.1116/1.574016

[5] R.L. Aggarwal, J.K. Furdyna, S. von Moln, Diluted Magnetic (Semimagnetic) Semiconductors, In Materials Research Society Symposia Proceedings, Pittsburgh, PA, 89, 97 (1987).

[6] H. Ambreen, S. A. Aldaghfag, M. Yaseen, J. Iqbal, M. Zahid, A. Dahshan, H. H. Hegazy, Physica Scripta, 97(6), 065807 (2022); https://doi.org/10.1088/1402-4896/ac6910

[7] S.W. Fan, L.J. Ding, K.L. Yao, Journal of Applied Physics, 114(11), 113905 (2013); https://doi.org/10.1063/1.4821261

[8] T. Dietl, H. Ohno, F. Matsukura, J. Cibert, D. Ferrand, Science 287,1019-1022 (2000); https://doi.org/10.1126/science.287.5455.1019

[9] R.A. de Groot, F.M. Mueller, P.G. van Engen, K.H.J. Buschow, Phys. Rev. Lett. 50, 2024-2027 (1983); https://doi.org/10.1103/PhysRevLett.50.2024

[10] R.J. Soulen Jr., J.M. Byers, M.S. Osofsky, B. Nadgorny, T. Ambrose, A. Barry, J.M.D.Coey, Science 282, 85 (1998); https://doi.org/10.1126/science.282.5386.85

[11] I. Galanakis, 2005. Physical Review B, 71(1), 012413; https://doi.org/10.1103/PhysRevB.71.012413

[12] K.I. Kobayashi, T. Kimura, H. Sawada, K. Terakura, Y. Tokura, Nature, 395(6703), 677-680 (1998); https://doi.org/10.1038/27167

[13] H. Saito, V. Zayets, S. Yamagata, K. Ando, Journal of applied physics, 93(10), 6796-6798 (2003); https://doi.org/10.1063/1.1556117

[14] S. Picozzi, T. Shishidou, A.J. Freeman, B. Delley, Physical Review B, 67(16), 165203 (2003); https://doi.org/10.1103/PhysRevB.67.165203

[15]. M. Sajjad, H. X. Zhang, N. A. Noor, S. M. Alay-e-Abbas, M. Younas, M. Abid, A. Shaukat, Journal of Superconductivity and Novel Magnetism, 27(10), 2327-2336 (2014); https://doi.org/10.1007/s10948-014-2593-1

[16] M.E.A. Monir, A. Bahnes, A. Boukortt, A.B. Reguig, Y. Mouchaal, Journal of Magnetism and Magnetic Materials, 497, 166067 (2020); https://doi.org/10.1016/j.jmmm.2019.166067

[17] M.E.A. Monir, H. Baltache, G. Murtaza, R. Khenata, W.K. Ahmed, A. Bouhemadou, S.B. Omran, T. Seddik, Journal of Magnetism and Magnetic Materials, 374, 50-60 (2015); https://doi.org/10.1016/j.jmmm.2014.08.014

[18] M.E.A. Monir, H. Baltache, R. Khenata, G. Murtaza, S. Azam, A. Bouhemadou, Y. Al-Douri, S.B. Omran, R. Ali, Journal of Magnetism and Magnetic Materials, 378, 41-49 (2015); https://doi.org/10.1016/j.jmmm.2014.10.070

[19] S. Levcenco, D.O. Dumcenco, Y.P. Wang, J.D. Wu, Y.S. Huang, E. Arushanov, V. Tezlevan, K.K. Tiong, Optical Materials, 34(7), 1072-1076 (2012); https://doi.org/10.1016/j.optmat.2012.01.004

[20] T. Ebisawa, I. Nomura, K. Kishino, K. Tasai, H. Nakamura, T. Asatsuma, H. Nakajima, Journal of crystal growth, 311(8), 2291-2293 (2009); https://doi.org/10.1016/j.jcrysgro.2009.01.123

[21] I. Nomura, K. Kishino, T. Ebisawa, Y. Sawafuji, R. Ujihara, K. Tasai, H. Nakamura, T. Asatsuma, H. Nakajima, Applied Physics Letters, 94(2) 021104 (2009); https://doi.org/10.1063/1.3058761

[22] Y. Nakai, I. Nomura, Y. Takashima, A. Kikuchi, K. Kishino, Physica Status Solidi (A),

201(12), 2708-2711 (2004); https://doi.org/10.1002/pssa.200405106

[23] H. Ambreen, S. A. Aldaghfag, M. Yaseen, M. Zahid, H. H. Somaily, Physica Scripta, 97(4), 045702 (2022); https://doi.org/10.1088/1402-4896/ac58cd

[24] A. Munoz, P. Rodríguez-Hernández, A. Mujica, Physica Status Solidi (B), 198(1), 439-446 (1996); https://doi.org/10.1002/pssb.2221980157

[25] A. Munoz, P. Rodriguez-Hernandez, A. Mujica, Physical Review B, 54(17), 11861 (1996); https://doi.org/10.1103/PhysRevB.54.11861

[26] H. S. Saini, Poonam, A. K. Pundir, M. Singh, J. Thakur, M. K. Kashyap, AIP Conference Proceedings, 2115(1), 030498 (2019); https://doi.org/10.1063/1.5113337

[27] Q. Mahmood, S.M. Alay-e-Abbas, A. Mahmood, M. Yaseen, I. Mahmood, N.A. Noor, Journal of Superconductivity and Novel Magnetism, 29, 521-530 (2016); https://doi.org/10.1007/s10948-015-3330-0

[28] C.M.I. Okoye, Euro. Phys. J. Cond. Matter Compl. Sys. 39(1), 5 (2004); https://doi.org/10.1140/epjb/e2004-00164-3

[29] N.A. Noor, S.M. Alay-e-Abbas, Y. Saeed, S.G. Abbas, A. Shaukat, Journal of magnetism and magnetic materials, 339, 11-19 (2013); https://doi.org/10.1016/j.jmmm.2013.02.040

[30] H. Ambreen, M. Yaseen, A. Ghaffar, M. Zahid, Materials Science in Semiconductor Processing, 127, 105697 (2021); https://doi.org/10.1016/j.mssp.2021.105697

[31] S.M. Alay-e-Abbas, K.M. Wong, N.A. Noor, A. Shaukat, Y. Lei, Solid State Sciences, 14(10), 1525-1535 (2012); https://doi.org/10.1016/j.solidstatesciences.2012.08.020

[32] A. Benkada, S. Habri, B. N. Eddine, D. Bensaid, M. Hamli, B. Kaddour, The European Physical Journal B, 94(5), 1-9 (2021); https://doi.org/10.1140/epjb/s10051-021-00106-x

[33] M. Yaseen, H. Ambreen, M. Zia, H. M. Javed, A. Mahmood, A. Murtaza, Journal of Superconductivity and Novel Magnetism, 34(1), 135-141 (2021); https://doi.org/10.1007/s10948-020-05674-0

[34] M. Yaseen, M. Dilawar, H. Ambreen, S. Bibi, S. U. Rehman, U. Shahid, M. Khalid Butt, A. Ghaffar, A. Murtaza,Bulletin of Materials Science, 43(1), 1-8 (2020); https://doi.org/10.1007/s12034-020-2078-8

[35] S. Saleem, M. Yaseen, S. A. Aldaghfag, R. Neffati, Physica Scripta, 97(9), 095817 (2022); https://doi.org/10.1088/1402-4896/ac8a27

[36] S. Chattopadhyaya, R. Bhattacharjee, Journal of Physics and Chemistry of Solids, 100, 57-70 (2017); https://doi.org/10.1016/j.jpcs.2016.09.005

[37] N. A. Noor, S. M. Alay-e-Abbas, Y. Saeed, S. G. Abbas, A. Shaukat, Journal of magnetism and magnetic materials, 339, 11-19 (2013); https://doi.org/10.1016/j.jmmm.2013.02.040

[38] H. Baaziz, Z. Charifi, F. El Haj Hassan, S. J. Hashemifar, H. Akbarzadeh, physica status solidi (b), 243(6), 1296-1305 (2006); https://doi.org/10.1002/pssb.200541481

[39] Q. Mahmood, B.U. Haq, M. Yaseen, A. Shahid, A. Laref, Solid State Commun. 299, 113654 (2019); https://doi.org/10.1016/j.ssc.2019.113654

[40] S. Berri, Journal of Science: Advanced Materials and Devices, 3(2), 254-261 (2018); https://doi.org/10.1016/j.jsamd.2018.03.001

[41] A.M. Shawahni, M.S. Abu-Jafar, R.T. Jaradat, T. Ouahrani, R. Khenata, A. A. Mousa, K.F. Ilaiwi, Materials 11(10) 2057 (2018); https://doi.org/10.3390/ma11102057

[42] M. Hassan, N. Akhtar, Q. Mahmood, A. Laref, Materials Science and Engineering: B, 238, 50-60 (2018); https://doi.org/10.1016/j.mseb.2018.12.006

[43] N. A. Noor, W. Tahir, F. Aslam, A. Shaukat, Physica B: Condensed Matter, 407(6), 943-952 (2012); https://doi.org/10.1016/j.physb.2011.12.107

[44] D.R. Penn, Phys. Rev. 128, 2093-2097 (1962);
https://doi.org/10.1103/PhysRev.128.2093

[45] M. A. Khan, H. A. Alburaih, N. A. Noor, A. Dahshan, Solar Energy, 225, 122-128 (2021);
https://doi.org/10.1016/j.solener.2021.07.026

[46] F. Aslam, H. Ullah, M. Hassan, Materials Science and Engineering: B, 274, 115456 (2021);
https://doi.org/10.1016/j.mseb.2021.115456

[47] F. Zareef, M. Rashid, A.A.H. Ahmadini, T. Alshahrani, N.A. Kattan, A. Laref, Mater. Sci. Semicond. Process. 127, 105695 (2021);
https://doi.org/10.1016/j.mssp.2021.105695

[48] S.A. Aldaghfag, M. Yaseen, H. Ambreen, M.K. Butt, M. Rehan, A. Dahshan, Chalcogenide Letters, 18(7), 357-365 (2021).

[49] G.K. Madsen, D.J. Singh, BoltzTraP: Comp. Phys. Commun. 175, 67-71 (2006).
https://doi.org/10.1016/j.cpc.2006.03.007
https://doi.org/10.1016/j.cpc.2006.03.007